Assimilation of Active and Passive Microwave Observations for Improved Estimates of Soil Moisture and Crop Growth

Pang-Wei Liu, *Member, IEEE*, Tara Bongiovanni, Alejandro Monsivais-Huertero, *Senior Member, IEEE*, Jasmeet Judge, *Senior Member, IEEE*, Susan Steele-Dunne, Rajat Bindlish, *Senior Member, IEEE*, and Thomas J. Jackson, *Fellow, IEEE*

***Abstract*—An ensemble Kalman Filter-based data assimilation framework that links a crop growth model with active and passive (AP) microwave models was developed to improve estimates of soil moisture (SM) and vegetation biomass over a growing season of soybean. Complementarities in AP observations were incorporated to the framework, where the active observations were used to optimize surface roughness and update vegetation biomass, while passive observations were used to update SM. The framework was implemented in a rain-fed agricultural region of the southern La-Plata Basin during the 2011–2012 growing season, through a synthetic experiment and AP observations from the Aquarius mission. The synthetic experiment was conducted at a temporal resolution of 3 and 7 days to match the current AP missions. The assimilated estimates of SM in the root zone and dry biomass were improved compared to those from the cases without assimilation, during both 3- and 7-day assimilation scenarios. Particularly, the 3-day assimilation provided the best estimates of SM in the near surface and dry biomass with reductions in RMSEs of 41% and 42%, respectively. The absolute differences of assimilated LAI from Aquarius were < 0.29 compared to the MODIS LAI indicating that the performance of assimilation was similar to the MODIS product at a regional scale. This study demonstrates the potential of assimilation using AP observations at high temporal resolution such as those from soil moisture active passive (SMAP) for improved estimates of SM and vegetation parameters.**

***Index Terms*—Active microwave remote sensing, aquarius, data assimilation, passive microwave remote sensing, soil moisture (SM), soil moisture active passive (SMAP).**

Manuscript received March 15, 2015; revised November 19, 2015; accepted December 01, 2015. Date of publication January 06, 2016; date of current version March 11, 2016. This work was supported by the NASA-Terrestrial Hydrology Program (THP-NNX09AK29G), in part by the Netherlands Organization for Scientific Research (NWO) Veni Grant Program (ALW 863.09.015), and in part by the National Council of Science and Technology of Mexico (CB-2010-155375).

P.-W. Liu, T. Bongiovanni, and J. Judge are with the Center for Remote Sensing, Department of Agricultural and Biological Engineering, Institute of Food and Agricultural Sciences, University of Florida, Gainesville, FL 32611 USA (e-mail: bonwei@ufl.edu).

A. Monsivais-Huertero is with ESIME Ticomán/CDA, National Polytechnic Institute, Mexico City 07738, Mexico.

S. Steele-Dunne is with the Department of Water Management, Delft University of Technology, Delft 2628, The Netherlands.

R. Bindlish and T. J. Jackson are with the U.S. Department of Agriculture, Agricultural Research Center Hydrology, and Remote Sensing Laboratory, Beltsville, MD 20705 USA.

Color versions of one or more of the figures in this paper are available online at http://ieeexplore.ieee.org.

Digital Object Identifier 10.1109/JSTARS.2015.2506504

I. Introduction

ACCURATE estimates of crop development over a growing season are important for managing agricultural production and assessing food security. Dynamic crop simulation models, such as decision support system for agrotechnology transfer (DSSAT) model, can be used to estimate crop growth as well as soil moisture (SM) [1], [2]. However, these estimates may diverge from reality over time due to errors in computation, initial conditions, forcing data, and model parameters. Auxiliary information may be incorporated into these dynamic models to improve estimations through data assimilation. Soil moisture is a critical factor governing the energy and water fluxes, and is one of the most dominant variables for crop growth processes [3]. Assimilating SM or remotely sensed observations that are sensitive to SM in the dynamic crop growth model improves the estimation of crop growth parameters, such as biomass accumulation, over the growing season, and thus the prediction of crop yield [4], [5].

Microwave observations have been widely used for estimates of water contained in the soil because the relaxation frequency of water lies in the microwave region (0.3–300 GHz), resulting in a significant difference in dielectric constant between dry and wet soils. Observations at L-band (1–2 GHz) are preferable due to lower attenuation by clouds and vegetation [6], [7]. Current satellite-based microwave missions provide global scale microwave observations at L-band that can be used for data assimilation. For instance, the soil moisture ocean salinity (SMOS) mission, operated by the European Space Agency (ESA), provides passive observations at 1.41 GHz (L-band) at 25–50 km every 2–3 days [8]. The National Aeronautics and Space Administration and Comisión Nacional de Actividades Espaciales (NASA/CONAE)-Aquarius mission provides synchronous L-band active and passive (AP) observations at 1.26 and 1.41 GHz, respectively, at a spatial resolution of 100 km with repeat coverage of 7 days [9], [10]. The recently launched NASA soil moisture active passive (SMAP) mission will provide AP observations at 1.26 and 1.41 GHz at the spatial resolutions of 3 and 36 km, respectively, with a repeat coverage of 2–3 days [7].

Over the last two decades, studies have been done for retrieving near-surface SM from microwave observations either using inversion of physically based model (e.g., [11], [12]) or more recently, using data driven techniques such as Bayesian, neural network, or support vector regression (e.g., [13]–[15]). This

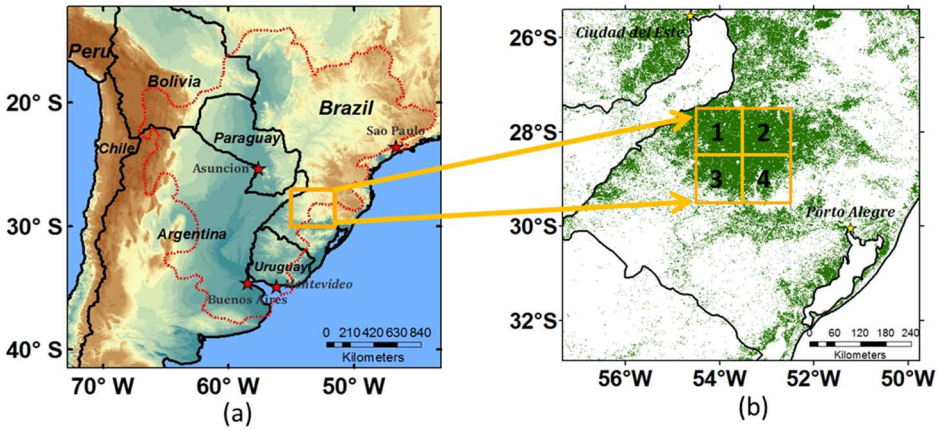

Fig. 1. (a) Geographical location of the LPB, delineated as red line, in South America. (b) Land cover map with four Aquarius pixels in the study region. The green dots indicate agricultural fields at spatial resolution of 1 km.

retrieved SM can be propagated through the root zone by incorporating biophysically based models with assimilation. Significant progress has been made to improve estimates of root zone SM (RZSM) and crop development from the hydrologic (e.g., [16]–[18]) and crop growth models (e.g., [4], [19], [20]) by assimilating near-surface SM. However, errors may be introduced in retrieved SM products due to parameter uncertainties in retrieval algorithms that may affect the performance of assimilation algorithm. Instead, assimilating microwave observations directly by using a crop model linked with forward microwave models may avoid such errors [5].

A few studies assimilated either active or passive observation in the crop growth or land surface process (LSP) models [5], [21]. For example, Prévot *et al.* [5] coupled the STICS crop model with the radiative transfer (RT) equation to assimilate radar observations (σ^0) at C-band to improve the prediction of biomass accumulation of wheat. Nagarajan *et al.* [21] assimilated brightness temperature (T_B) at L-band in the linked LSP with DSSAT model to improve estimates of RZSM during a growing season of sweet corn. Even though both AP microwave observations are sensitive to the SM in the near surface [22], the passive observation of T_B is more sensitive to SM but less sensitive to surface roughness and vegetation compared to the active observation of radar backscattering (σ^0). Utilizing complementarities of the two observations could improve estimates of SM and vegetation water content (VWC) [23]. Studies using AP observations for data assimilation in hydrologic models are rare [18], [24]. Typically, these studies have been conducted for a short time period and the vegetation properties were assumed constant. A gap remains in the development of physically based methodologies that integrate the complementary information from AP observations of σ^0 and T_B, into a data assimilation framework to improve the estimation of SM and vegetation growth over a growing season.

The goal of this study is to improve the estimation of SM and crop growth utilizing the complementarities of AP observations. The objectives of this study are to 1) develop and evaluate an ensemble Kalman filter (EnKF)-based assimilation framework that integrates AP observations with a linked DSSAT-microwave model, using a synthetic experiment; and 2) implement the framework to assimilate the real satellite-based AP observations from the Aquarius in an agricultural region. This study provides insights into data assimilation using synchronous AP observation such as those from the Aquarius and SMAP missions.

II. Study Area and Data Products

A. Study Region

The La Plata Basin (LPB) is one of the largest basins on the earth, covering parts of Argentina, Bolivia, Brazil, Paraguay, and Uruguay, and is considered as the most economically important agricultural region for these countries. This study was conducted in a region with an area of about 200 km $\times$ 200 km in the lower LPB in Brazil, as shown in Fig. 1(a). The soils in the region are oxisols with clayey texture of 30%–60% clay [25], and the predominant crop in this region is soybean with a rain-fed agricultural system. This rain-fed region is vulnerable to high losses in crop yields due to agricultural drought which is predicted to continue under warmer and drier climate. Therefore, it is essential to accurately predict the crop yield in this region to manage food production and security.

B. Weather Forcing Data for DSSAT Model

This study was conducted during a growing season of soybean from November 15 [day of year (DOY) 319] 2011 to March 30 (DOY 90) 2012. The weather forcing data used in this study, including precipitation (PPT), solar radiation (R-Solar), maximum and minimum air temperature, dew point, and wind speed, were obtained from satellite-based products and models, as listed in the Table I. Both the PPT and R-Solar were spatially averaged to 100 km $\times$ 100 km corresponding to the spatial resolution of the AP observations used in this study. The R-Solar was temporally averaged, while the PPT was accumulated over the 24-h period to daily forcing data for DSSAT model.

C. AP Observations From Aquarius for Assimilation

Gridded observations of σ^0 and T_B at the spatial resolution of 100 km $\times$ 100 km from Aquarius version 2.0 [10], [26] were assimilated into the data assimilation framework. The

TABLE I
WEATHER FORCING FROM SATELLITE-BASED PRODUCTS AND MODELS FOR DSSAT MODEL

Products	Satellite mission	Original resolution	Temporal resolution
Precipitation	TRMM[1]	0.25^o	3 h
Solar radiation	GOES (GSIP)[2]	12.5 km	3 h
Max. & Min. temperature	NASA-POWER[3]	100 km	Daily
Dew point	NASA-POWER	100 km	Daily
Wind speed	NASA-POWER	100 km	Daily

[1]Tropical Rainfall Measuring Mission.
[2]Geostationary Operational Environmental Satellite (GOES Surface and Insolation Product).
[3]NASA-Prediction of Worldwide Energy Resource.

observations from the second beam of Aquarius, at an incidence angle of 38.5°, at 6 A.M. local time (descending orbit), were used to avoid varying scattering mechanisms due to different incidence angles. In addition, such an incidence angle is close to the SMAP mission, so the performances of the assimilation algorithm may provide insights into the SMAP mission. The study region consisted of four Aquarius pixels, and the two pixels in the north were primarily agricultural (>92%), as shown in Fig. 1(b). In this study, the two pixels in the north were used to test the assimilation framework.

D. LAI Product for Evaluation of Assimilation Performance

Leaf area index (LAI) from MODIS was used to compare with that from assimilation using Aquarius observations. Only MODIS pixels classified as agricultural land use within the region were considered and averaged, so errors from the nonagricultural pixels were minimized.

III. MODELS

A. DSSAT Model

The DSSAT is a crop growth model that simulates biomass accumulation and phenological development at a daily time step for a variety of crops in different hydro-climate regions [1], [27]–[35]. The model consists of modules for crop development and growth, weather, soil, and soil–plant–atmosphere [1]. In this study, the DSSAT-CROPGRO soybean module [2] was used to simulate the phenological development and growth of soybean. Vegetation parameters were obtained from existing cultivars in the DSSAT V4.5 database. The soil module uses a one-dimensional (1-D) tipping bucket model to simulate soil water transport [36], and models the soil temperature as an empirical function of air temperature and depth. In this study, the soil was divided into two layers, 0–5 and 5–120 cm. The hydraulic parameters of the soil, such as wilting point, drainage rate, field capacity, porosity, and hydraulic conductivity, were estimated from soil-water characteristic models [37] using published soil textures obtained from field measurements [38]–[42]. Other soil parameters, such as albedo and organic mater content, were obtained from the DSSAT V4.5 soils database for the region [1]. The soil–plant–atmosphere module estimates evapotranspiration, and the weather module simulates and reads the meteorological forcing data. The soil moisture, temperature, and vegetation characteristics provided by the DSSAT model were used in the AP forward models to estimate σ^0 and T_B.

B. Backscatter Model

The backscatter from a vegetated terrain ($\sigma^0_{terrain}$) is modeled as

$$\sigma^0_{terrain} = \gamma^2 \sigma^0_{soil} + \sigma^0_{veg} + \sigma^0_{int} \tag{1}$$

where σ^0_{soil} represents the direct backscatter contribution of the underlying soil surface, γ^2 is the two-way transmissivity of the canopy, σ^0_{veg} is the direct backscatter from the soybean canopy, and σ^0_{int} is the interaction between canopy and soil.

During the bare soil, a physically based model, the advanced integral equation model (AIEM) [43], was used to estimate the radar backscattering coefficient from the soil, due to its applicability for a wide range of roughness and frequencies. The AIEM provides backscattering of the soil as a function of incidence angle (θ_0), frequency (f), dielectric constant of wet soil (ϵ), and surface roughness. In this study, the σ^0_{soil} was estimated at a θ_0 of 38.5° and a frequency of 1.26 GHz to match the active observations of the Aquarius mission. The ϵ was estimated using soil moisture from the DSSAT model through a mineralogically based model [44].

During the growing season, the Michigan microwave canopy scattering (MIMICS) model [45] was used to estimate the canopy extinction σ^0_{veg} and σ^0_{int} in soybean. The model was linked with the AIEM for the backscattering contribution from the soil. The MIMICS model is based on the RT theory and calculates radar backscattering from vegetation by balancing the amplitudes of incoming and outgoing energies across an elemental volume. The MIMICS model, originally developed for forest, was adapted to soybean, where the soybean was modeled as a single-layer vegetation medium with one class of cylindrical stems and one class of disc leaves [46]–[49]. Vegetation parameters in the MIMICS model include moisture content, number density, and geometrical description of stems and leaves. Because the DSSAT model estimates dry biomass of leaves ($B_{D,leaf}$) and stems ($B_{D,stem}$), an empirical function [50], as shown in (2), was used to estimate their fresh biomass, i.e., $B_{W,leaf}$ and $B_{W,stem}$

$$B_{W,leaf/stem} = \frac{B_{D,leaf/stem}}{0.5G^2[-0.084 + 0.032ln(G)] + 0.099G + 0.0196} \tag{2}$$

where G is the phenological growth stage obtained from the DSSAT model. The values of G are from 0 to 8, from vegetative to full maturity, as detailed in [51]. The VWC of leaf and stem VWC_{leaf} and VWC_{stem} were directly obtained by subtracting

TABLE II
VEGETATION PARAMETERS USED IN THE MIMICS MODEL

	Parameters	Description
Canopy	Height (m): H_t	From DSSAT
Stems	Height (m): SH_t	Function of H_t in [47]
	Diameter (m): SD	Function of H_t in [47]
	Fresh biomass (kg/m^2): $B_{W,stem}$	Function of G and $B_{D,stem}$ as in Eq. (2)
	Vegetation water content (kg/m^2): VWC$_{stem}$	$B_{W,stem}-B_{D,stem}$
	Density (#/m^3): Sden	$40/H_t$
	Euller angle α (°)	0–360
	Euller angle β (°)	0–10
Leaves	Thickness (m): LT	0.001
	Diameter (cm): LR	Function of LAI in [47]
	Fresh biomass (kg/m^2): $B_{W,leaf}$	Function of G and $B_{D,leaf}$ as in Eq. (2)
	Vegetation water content (kg/m^2): VWC$_{leaf}$	$B_{W,leaf}-B_{D,leaf}$
	Density (#/m^3): Lden	Sden $\times$ number of leaves per plant from DSSAT
	Euller angle α (°)	0–360
	Euller angle β (°)	0–15

their dry biomass from fresh biomass. Other input parameters were obtained either from DSSAT model or through empirical relationships between different parameters [47]. Details of stem and leaf parameters used in this study are listed in the Table II.

C. Microwave Emission Model (MB)

Brightness temperature from a vegetated terrain ($T_{Bterrain}$) is modeled as the sum of contributions from soil (T_{Bsoil}) and vegetation (T_{Bveg}) as follows:

$$T_{Bterrain} = T_{Bsoil} + T_{Bveg} \tag{3a}$$

$$T_{Bsoil} = e \cdot T_{eff} \cdot e^{(-\tau sec\theta_0)} \tag{3b}$$

$$T_{Bveg} = T_c \cdot \left[1 - e^{(-\tau sec\theta_0)}\right](1-\omega)\left[1 + r \cdot e^{(-\tau sec\theta_0)}\right] \tag{3c}$$

where T_{eff} is the effective temperature of bare soil estimated using first-order approximation [52], e refers to soil emissivity estimated using the integral form of AIEM [43], r is the soil reflectivity equivalent to $(1-e)$, τ is the vegetation opacity as a function of frequency, VWC, and B_W of vegetation medium using the cloud density model [53], ω is the single-scattering albedo that is typically considered to be low at L-band and was ignored in this study [54], and T_c is the physical temperature of the canopy, which is assumed isothermal and equal to air temperature [55].

The $T_{Bterrain}$ was estimated at 1.41 GHz matching the passive observations of the Aquarius mission. The θ_0 and ϵ used in the MB model were the same as those used in the backscatter model described in Section III-B. The total VWC and B_W of soybean for the MB model were obtained by combining VWC_{stem} and VWC_{leaf}, and $B_{W,stem}$ and $B_{W,leaf}$, respectively, as mentioned in the Section III-B.

D. Ensemble Kalman Filter

In this study, we utilized an EnKF-based assimilation framework that uses a Monte Carlo approach to obtain optimized means and covariances of states over time and to merge them with the observations when available. In the framework, a set of ensemble members representing state vectors is propagated in parallel, such that each state vector represents one realization of all model simulations. The state equation in the EnKF for each ensemble member is [56]

$$x_t^{i-} = f\left(x_{t-1}^{i+}, u_{t-1}^i, \theta_{t-1}^+, t-1\right) + \eta_{t-1}^i \tag{4}$$

where $f(\cdot)$ is the nonlinear model, x_t^{i-} is the state of the ith ensemble prior to the update at time t, x_{t-1}^{i+} is the posterior state of the ith ensemble at time $t-1$, u_{t-1}^i represents the meteorological forcing data, θ_{t-1}^+ represents the model parameters, and η_{t-1}^i is the model error. In this study, the model physics were assumed to be perfect, i.e., $\eta_{t-1}^i = 0$, and the uncertainties in meteorological forcings and model parameters are described in the Section IV-C.

The observation equation given in (5) relates the prior state (x^{i-}) to the observations (d^i) through the measurement operator M [24], with additive Gaussian errors (ω) at time t

$$d_t^i = M(x_t^{i-}) + \omega_t^i \tag{5}$$

In this study, the measurement operators were the radar backscatter and MB models, that relate the SM and vegetation characteristics from DSSAT model to the AP observations.

The ensemble of state vectors x^i and perturbed observations d^i can be represented in matrix forms as

$$A = \{x^1, x^2, \ldots, x^N\} \tag{6}$$

$$D = \{d^1, d^2, \ldots, d^N\} \tag{7}$$

where N is the number of ensemble members.

The posterior matrix of the state vectors, A_t^+ is computed as a linear combination of the estimates from the measurement operator using the prior estimate $M(A_t^-)$ and the observation vector D_t weighed by the Kalman gain K_t given as [57]

$$A_t^+ = A_t^- + K_t(D_t - M(A_t^-)) \tag{8a}$$

$$K_t = A_t' M(A_t^-)^T \left(M(A_t^-)M(A_t^-)^T + R_e\right)^{-1} \tag{8b}$$

where A_t' is the matrix of $A_t^- - \bar{A}_t^-$, and R_e is the covariance matrix of the observation errors, defined as $R_e = \gamma\gamma^T$, where γ is the ensemble of observation error.

TABLE III
SOIL PARAMETERS FOR DSSAT AND AP MODELS

Parameter	Range
Wilting point (m^3/m^3)	0.179–0.343
Field capacity (m^3/m^3)	0.311–0.493
Saturated hydraulic conductivity (cm/hr)	0.127–0.587
Porosity (m^3/m^3)	0.494–0.555
Drainage rate (fraction/day)	0.021–0.912
RMS height (m): s	0.005–0.015
Correlation length (m): l	0.045–0.150

TABLE IV
ERRORS IN WEATHER FORCING DATA

Parameter	Std.
Max. temperature	3.9 K
Min. temperature	1.6 K
Wind speed	1 m/s
Dew point	3.65 K
Precipitation	12%
Solar radiation	10%

IV. METHODOLOGY

In this section, we describe the simulation using DSSAT coupled with the forward backscatter and MB models (DSSAT-AP) and implementation of the assimilation framework that incorporates complementarities of AP observations using the EnKF.

A. DSSAT-AP Simulation

The simulations using the uncalibrated DSSAT-AP model started on DOY 245, 2011, 2.5 months before planting. The soybean was planted on DOY 319, 2011 and harvested on DOY 90, 2012. Fifty realizations of DSSAT-AP model without assimilation, i.e., an ensemble open loop, were conducted at a daily time step for the 212 days including bare soil and the soybean growing season. The initial SM and temperatures were the same for both the soil layers and for all the ensemble members. The initial SM was the seasonal mean of the maximum and minimum SM from Aquarius, and the initial soil temperature was estimated from the DSSAT soil module using the maximum and minimum air temperatures at the start of the simulation. The soybean growing season in 2011–2012 was relatively dry with a total PPT of 389 mm in this region. The soybean plant density was 40 plants per m^2 with a row spacing of 0.45 m [58]. The soil consists of 0.3–0.6 by volume of clay and 0.03–0.45 by volume of sand in this region, and constitutive properties were obtained from [37], as shown in Table III. The daily meteorological forcing data were obtained from satellite-based products and models as mentioned in Section II, and Gaussian errors were introduced in all weather forcing data as listed in the Table IV.

The vegetation parameters were obtained from four cultivars in DSSAT V4.5 within maturity groups 5 and 6 to preserve an interrelationship between cultivars. The dry biomass obtained from DSSAT was converted to wet biomass, VWC, and dimensions of leaf and stem for the backscatter and MB models, as mentioned in Sections III-B and III-C, and shown in Fig. 2(a)–(d). Overall, the estimates of VWC, $\mathrm{VWC_{leaf}}$, $\mathrm{VWC_{stem}}$, and LAI increase along with the growing season but vary over time because of the dynamic weather conditions. On day after planting (DAP) 110, the soybean seeds have reached their full size, dry biomass accumulation has ceased as leaf senescence continues, and the plant continues to dry down until harvest maturity is reached. The leaf diameter follows similar variation to the LAI because it was estimated by using an empirical equation from LAI. The stem height and diameter become stable on DAP 78, when the VWC reaches its highest value. The number density of stem is inversely proportional to the canopy height and becomes stable since DAP 40 when increase in the canopy height becomes moderate. The number density of leaf tends to stabilize since DAP 20 when the leaf number from DSSAT model becomes stable.

The surface roughness parameters, root mean square height (s), and correlation length (cl), shown in Table III, were obtained from long-term experimental measurements conducted during MicroWEX-5 through MicroWEX-11 [59] to represent a natural agricultural field for backscatter and MB models.

B. AP Assimilation Framework

The flow diagram of the AP assimilation framework is shown in Fig. 3. The assimilation algorithm uses an EnKF-based framework, with the nonlinear propagator $f(\cdot)$ in (4) representing the DSSAT model; x is the state vector consisting of either SM or SM and vegetation characteristics estimated by the DSSAT model during the bare soil period before emergence and the vegetated period after emergence, respectively; u_t is the vector of meteorological forcing data at time t and θ are the model parameters in the DSSAT model. During the period before vegetation emergence, SM estimated from DSSAT model were used to generate σ^0 from AIEM. The observed σ^0 values were used to obtain the optimal value of s using the objective function as defined in (9). The VV-polarized (VV-pol) observations were used in this study due to their greater sensitivity to SM and vegetation characteristics compared to HH-pol observations [60]

$$D_{\sigma^0}(s) = \|\sigma^0_{terrain} - \hat{\sigma^0}_{terrain}\| \tag{9}$$

where $\sigma^0_{terrain}$ and $\hat{\sigma^0}_{terrain}$ represent the observed and estimated $\sigma^0_{terrain}$, and D_{σ^0} is the absolute difference between $\sigma^0_{terrain}$ and $\hat{\sigma^0}_{terrain}$.

During this process, only s was estimated for each ensemble member until the D_{σ^0} reached the tolerance (< 0.01 dB). The optimized s from (9) was used in the MB model and $\mathrm{T_B}$ was assimilated to update SM in the two soil layers using EnKF. The H-pol observations were used due to its higher sensitivity to SM than V-pol. The state vector for assimilating $\mathrm{T_B}$ is composed of

$$x = \begin{bmatrix} VSM_{\text{0-5 cm}} \\ VSM_{\text{5-120 cm}} \end{bmatrix}. \tag{10}$$

The posterior SM was used to optimize the s iteratively, as shown in Fig. 3. Such process was conducted until the posterior SM converged, with the difference of SM between $j+1$th and jth iteration was less than 0.005 $\mathrm{m^3/m^3}$. The converged SM was used to re-initialize DSSAT model during the propagation phase.

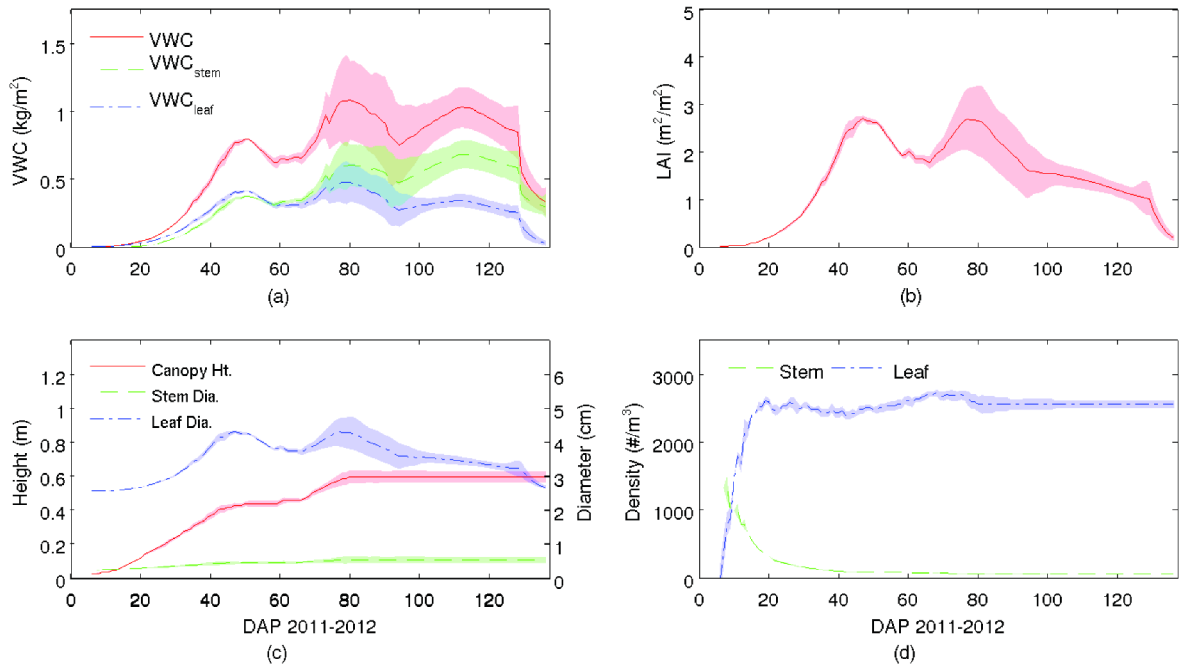

Fig. 2. Vegetation parameters from DSSAT model for backscatter and MB models during a growing season of soybean. (a) Total VWC and VWC of stem and leaf. (b) LAI. (c) Crop height and diameters of stem and leaf. (d) Vegetation number densities of stem and leaf. The bounded area represents one standard deviation of the parameters.

During the period after vegetation emergence, the σ^0_{VV} was assimilated to update the total dry biomass (B_D) and the $T_{B,H}$ was assimilated to update SM, as shown in Fig. 3. Although the σ^0_{VV} is more sensitive to the wet biomass, the B_D is a prognostic state in DSSAT model and the two wet biomass values are related by (2). The posterior B_D is provided to DSSAT model and the leaf, stem, and pod are obtained by preserving the prior ratio of biomass of each component. The state vector of an ensemble member for assimilating $T_{B,H}$ is the same as (10), while the state vector when assimilating σ^0_{VV} is expressed as

$$x = \left[B_D\right]. \tag{11}$$

The optimized value of s obtained during the period before vegetation was used for the entire vegetated period. Similarly, an iteration process was employed until the estimated SM converged, with the difference of SM between the $j+1$th and jth iteration is less than 0.005 m^3/m^3, and the optimized posterior dry biomass and SM were used to initialize DSSAT model for the next propagation phase.

C. Implementation of Assimilation

The synthetic experiment was conducted for the whole-study region consisting of four pixels. Fifty ($N = 50$) ensemble members were created for each pixel using perturbed forcing data and parameters for assimilation, as mentioned in Section IV-A and listed in Tables III and IV [20]. The synthetic truth was obtained from one of the realizations of the DSSAT-AP model. The synthetic AP observations were generated at a temporal resolution of 3 and 7 days, equivalent to 70 and 31 observations, respectively, over the period, matching the SMAP and Aquarius missions. Observations of $T_{B,H}$ and σ^0_{VV} in EnKF were obtained by perturbing the truth. The errors in AP observations were assumed Gaussian with zero mean and standard deviations of 3 K and 1 dB in T_{BH} and σ^0_{VV} [7], [21], respectively. The root mean square error (RMSE) between the mean estimates and the synthetic truth along with the time-averaged standard deviations of the mean estimates (ASD) were computed to evaluate the algorithm performance.

This study used Aquarius observations because they are the only simultaneous AP observations available for seasonally agricultural study currently. For the implementation of the assimilation using Aquarius observations, 2 pixels in the north that were homogeneous, as shown as pixels 1 and 2 in Fig. 1(b), were used. Thirty-one AP observations from Aquarius at each pixel over the study period of 212 days were assimilated using this framework. Significant biases in σ^0_{VV} and T_{BH}, of about 3 dB and 60 K, respectively, exist between the satellite-based observations and the open-loop simulations, as shown in the Fig. 4. These biases in observations were corrected prior to assimilation with respect to the seasonal mean [61], [62]. The AP observations of T_{BH} and σ^0_{VV} were perturbed by Gaussian errors, similar to the synthetic experiment. Because LAI largely correlates with the crop growth [63], the estimates of LAI from assimilation were compared to those from MODIS product, on DAP 30, 75, and 125, representing early-, mid-, and reproductive stages of soybean.

V. Results and Discussion

A. Synthetic Experiment

The assimilation results including three prognostic states $SM_{0-5\,\mathrm{cm}}$, $SM_{5-120\,\mathrm{cm}}$, and dry biomass, and a diagnostic

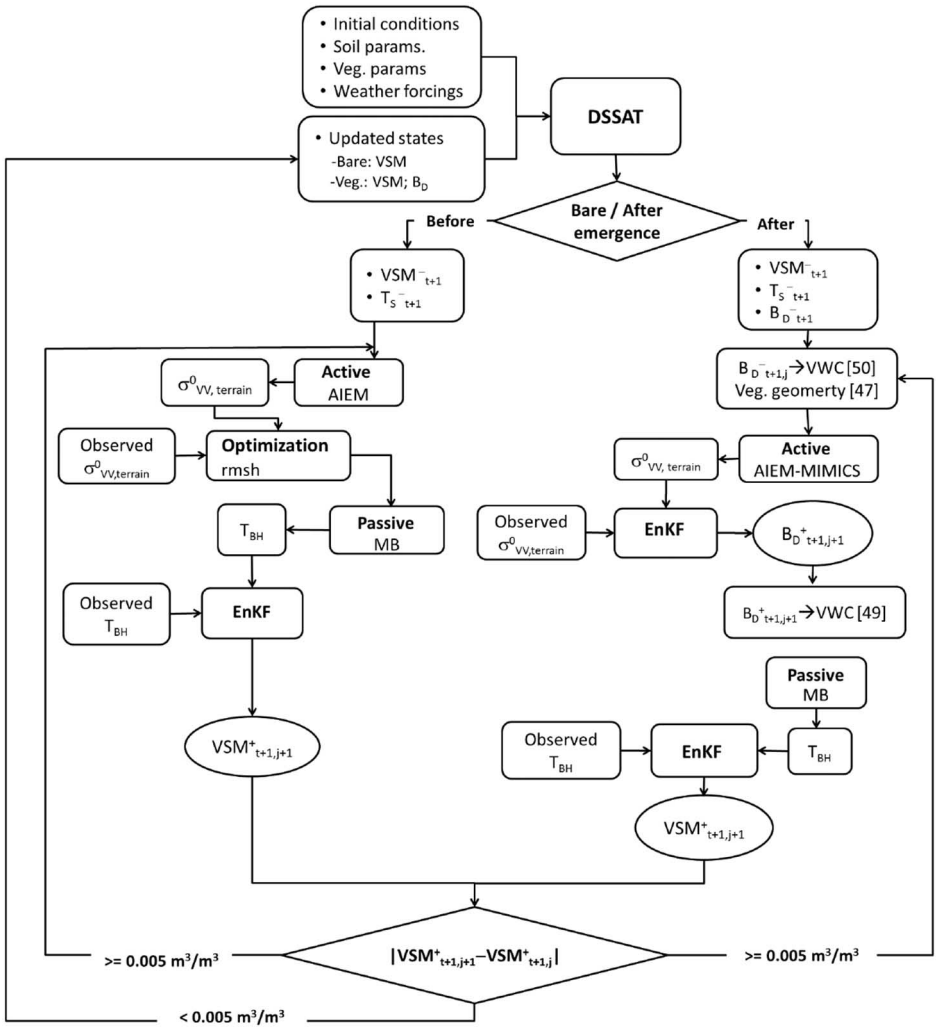

Fig. 3. Integration of DSSAT and AP forward models and assimilation flow diagram, where t represents the propagation phase at time t and j is the j th iteration at time t.

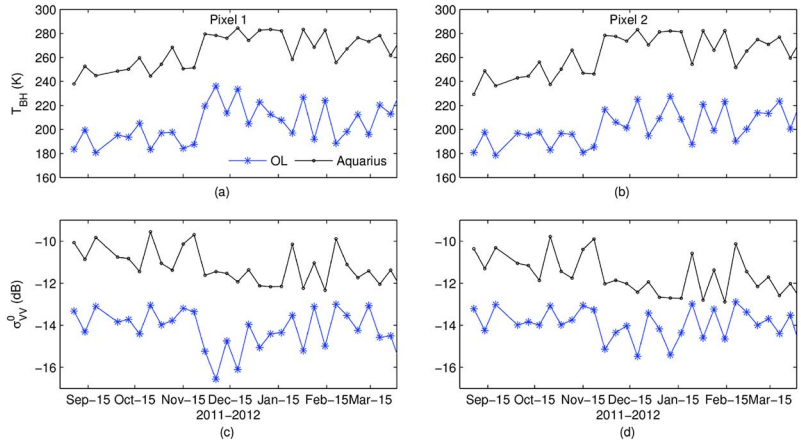

Fig. 4. Comparisons of AP observations between open loop simulations and Aquarius observations. (a) T_{BH} of pixel 1. (b) T_{BH} of pixel 2. (c) σ^0_{VV} from pixel 1. (d) σ^0_{VV} from pixel 2.

state LAI estimated from DSSAT model were compared to simulations from the open-loop and the synthetic truth. Before emergence, the mean rms slope (s/l) was optimized from 0.128 to 0.105, close to the synthetic truth at 0.106. Such an optimization in rms slope resulted in the estimated σ^0_{VV} approaching to the synthetic truth by as much as 2 dB. Fig. 5 shows scatterplots of three prognostic states from four pixels when the AP observations were assimilated. Overall, the EnKF-based framework significantly improves the estimations of the three prognostic states comparing to open-loop simulations by $>40\%$ in RMSE,

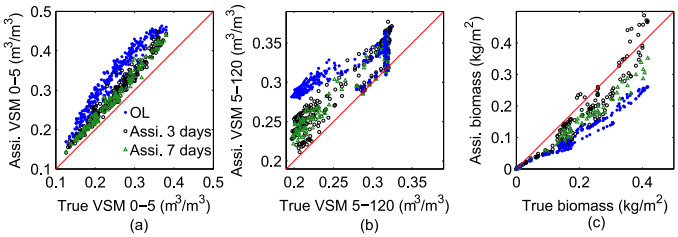

Fig. 5. Scatterplots of prognostic states when AP observations were assimilated. (a) $SM_{0-5\,\mathrm{cm}}$. (b) $SM_{5-120\,\mathrm{cm}}$. (c) Dry biomass.

TABLE V
RMSE OF $VSM_{0-5\,\mathrm{CM}}$, $VSM_{5-120\,\mathrm{CM}}$, AND DRY BIOMASS BETWEEN SYNTHETIC TRUTH AND OPEN LOOP, AND DATA ASSIMILATION WHEN THE AP OBSERVATIONS WERE ASSIMILATED

	$\mathrm{VSM_{0-5\,cm}}$ ($\mathrm{m^3/m^3}$)	$\mathrm{VSM_{5-120\,cm}}$ ($\mathrm{m^3/m^3}$)	$\mathrm{B_D}$ ($\mathrm{kg/m^2}$)
OL	0.086	0.058	0.091
7 days	0.036	0.031	0.058
3 days	0.040	0.034	0.045

as shown in Table V. Because the states were updated using the same methodology, as expected, the assimilations every 3 and 7 days performed similarly when the AP observations were assimilated.

Fig. 6 compares the truth, open-loop estimates, and the daily assimilated values of $SM_{0-5\,\mathrm{cm}}$, $SM_{5-120\,\mathrm{cm}}$, biomass, and LAI to evaluate the performance of assimilation framework over the growing season. The values were averaged over the four pixels in the region. The data assimilation either every 3 or 7 days significantly improves the estimations of the three prognostic states and the LAI over the season. Table VI shows the RMSE and ASD of the three prognostic states and LAI during periods before and after vegetation emergence, and the overall results for the whole period. The assimilation conducted every 3 days produced soil moisture estimates with lower RMSE compared to that conducted every 7 days. This indicates that the high temporal resolution of observations such as future SMAP mission or incorporating asynchronous observations from different satellite missions may further improve the assimilation under dynamic vegetation conditions. Particularly, improvements are more significant in $SM_{0-5\,\mathrm{cm}}$ and vegetation biomass using AP observations at higher temporal resolutions, because these are more dynamic states than $SM_{5-120\,\mathrm{cm}}$.

The estimates of dry biomass using assimilation every 3 and 7 days were significantly improved by 42% and 25% in RMSE, respectively, compared to the open loop. Although the RMSEs improved for estimates of dry biomass over the soybean growing season, ASDs increased by 76% and 42% from every 3- and 7-day assimilation, respectively, as shown in the Table VI, indicating larger uncertainties in the data assimilation. Similarly, the LAI estimates are improved by 20% and 18% compared to those from open loop, but the ASDs are increased by 63% and 41% from every 3- and 7-day assimilation, respectively. The higher uncertainties of dry biomass and LAI estimations from data assimilation resulted from the uncalibrated DSSAT model used in this study that causes unrealistic low estimates of dry biomass in some ensemble members. This suppressed plant growth due to low estimates of posterior SM conditions and caused the plants to die earlier than "normal" plants in the DSSAT model. That resulted in an increased uncertainty of vegetation estimations, including dry biomass and LAI. Thus, even though the data assimilation statistically improves the estimation of the vegetation biomass and LAI, the SD of biomass and LAI are increased.

Table VII shows the RMSEs of three soybean components from open loop and assimilation every 3 and 7 days. Estimates of leaves and stems biomass are improved by as much as 32% and 25%, respectively, but the RMSE of pods increased by as much as 82%. This suggests that the current backscatter model for soybean, which considers only leaves and stems, may be inadequate for the reproductive period when the volume of pods is significant and its contribution to backscattering may not be negligible. As a result, the estimate for pod biomass from data assimilation is underestimated. A more sophisticated radar backscatter model considering backscattering contributions from all three components is suggested for future study.

Results from data assimilation using AP observations showed improvements in updating dry biomass even though the microwave observations are physically more sensitive to vegetation wet properties such as VWC or wet biomass than dry properties. In this study, an empirical function from [50] was used to relate dry biomass to VWC for both backscatter and MB models, and, thus, the correlation between microwave observations to dry biomass was preserved. However, errors may be introduced due to uncertainties in the parameters from such an empirical function. Further modification in the DSSAT model is recommended in order to propagate wet biomass directly.

B. Assimilation of Aquarius Observations

The assimilation results of $SM_{0-5\,\mathrm{cm}}$, $SM_{5-120\,\mathrm{cm}}$, dry biomass, and LAI using AP observations from Aquarius are compared to their open loop values in Fig. 7. Table VIII shows the root mean square difference (RMSD) between open loop and data assimilation using AP observations from Aquarius and their ASDs. The ASDs of assimilated $SM_{0-5\,\mathrm{cm}}$ and $SM_{5-120\,\mathrm{cm}}$ are significantly reduced by 20% and 40%, respectively, but both ASDs of biomass and LAI are increased by 59%, similar to the synthetic experiment. The LAIs of two pixels from data assimilation are compared to those from MODIS on the DAP of 30, 75, and 125, as shown in Table IX. Overall, the LAIs estimated from data assimilation in this region are close to those from MODIS, with mean absolute difference (MAD) of 0.13, 0.29, and 0.25 $\mathrm{m^2/m^2}$ on the days of comparison. The uncertainties of LAI products from MODIS were found to be from 0.4 to 1.0 $\mathrm{m^2/m^2}$ for broad leaf crops such as soybean [64], [65]. According to the MAD values, there is not a significant difference between data assimilation using Aquarius observations and the LAI from MODIS product at the regional scale. Therefore, the assimilation using DSSAT-AP model and Aquarius does provide alternative for vegetation estimates at a regional scale particularly under cloudy conditions when remotely sensed observations from optical systems are not available.

The data assimilation using complementarities of AP observations improves the estimates of SM and dry biomass during

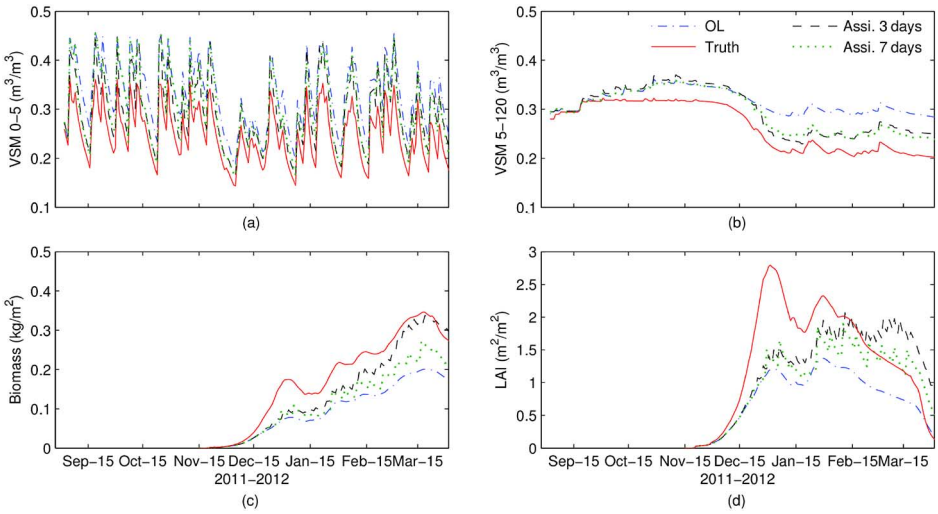

Fig. 6. Comparison of regional-averaged synthetic truth, open loop, and assimilated estimations every 3 and 7 days of (a) $SM_{0-5\,\mathrm{cm}}$; (b) $SM_{5-120\,\mathrm{cm}}$; (c) dry biomass; and (d) LAI.

TABLE VI
RMSE AND ASD OF $VSM_{0-5\,\mathrm{CM}}$, $VSM_{5-120\,\mathrm{CM}}$, BIOMASS, AND LAI BETWEEN SYNTHETIC TRUTH AND OPEN LOOP, AND DATA ASSIMILATION CONDUCTED EVERY 3 AND 7 DAYS

		$VSM_{0-5\,\mathrm{cm}}$ (m^3/m^3)		$VSM_{5-120\,\mathrm{cm}}$ (m^3/m^3)		B_D (kg/m^2)		LAI (m^2/m^2)	
		RMSE	ASD	RMSE	ASD	RMSE	ASD	RMSE	ASD
OL	BS	0.092	0.064	0.023	0.025	–	–	–	–
	Veg.	0.082	0.051	0.071	0.054	–	–	–	–
	Overall	0.086	0.056	0.058	0.043	0.092	0.075	0.766	0.635
7 days	BS	0.070	0.039	0.022	0.023	–	–	–	–
	Veg.	0.055	0.030	0.036	0.038	–	–	–	–
	Overall	0.061	0.034	0.032	0.032	0.069	0.095	0.625	0.899
3 days	BS	0.051	0.030	0.027	0.022	–	–	–	–
	Veg.	0.051	0.029	0.038	0.035	–	–	–	–
	Overall	0.051	0.030	0.034	0.030	0.053	0.132	0.616	1.036

BS and Veg. represent the periods before and after vegetation emergence, respectively.

TABLE VII
RMSES OF LEAVES, STEMS, AND PODS BIOMASS FROM OPEN LOOP AND DATA ASSIMILATION EVERY 3 AND 7 DAYS

	Leaves (kg/m^2)	Stems (kg/m^2)	Pods (kg/m^2)
OL	0.028	0.053	0.034
7 days	0.019	0.040	0.062
3 days	0.018	0.044	0.056

the crop growing season in the synthetic experiment. It should be noted that the implementation of an assimilation framework using observations from Aquarius assumes homogeneity at this coarse scale. Such an assumption may not be realistic for the agricultural applications and may introduce errors in the estimates. In order to further evaluate and assess the crop growth in this region, the AP observations from the SMAP mission and/or those derived through downscaling to finer spatial resolution at agricultural scale are recommended. In this study, the assimilation framework was implemented for synchronous AP observations available at the same spatial scale. The framework can be used for the SMAP AP observations by downscaling T_B from 36 to 9 km [55] and upscaling the σ^0 to the same spatial scale. To utilize the Level 1 AP observations from SMAP at different spatial resolution and consider the mixed pixels with different types of crop at the fine-scale active observations, the framework would need modifications by redesigning the observation matrix in the EnKF [24]. Besides, the Aquarius mission provides repeat observations every 7 days, which may also limit the performance of data assimilation. The SMAP providing AP observations every 3 days will significantly improve the performance of assimilation under highly dynamic SM and vegetation conditions.

This study also provided insights into the different vegetation opacity values in the active and the passive microwave models that may help to improve the performance of the assimilation algorithms. In this study, the vegetation opacity in the MIMICS model (τ_{MIMICS}) can be obtained using $\gamma{=}\exp(-\tau \sec\theta_0)$, where the γ was calculated using the Foldy's approximation that considers both scattering and absorption losses [45]. However, the vegetation opacity in the MB model (τ_{MB}) was obtained using the cloud density model that considers only absorption losses. These two opacity values are inconsistent, as shown in Fig. 8, because of different loss mechanisms in the two models. The τ_{MIMICS} was greater than τ_{MB} by as much as 0.02 over the soybean growing season. Such an inconsistency would not affect the assimilation results in the synthetic study because the AP observations were model-generated and follow model biophysics. However, the assimilation results using actual AP observations may be affected if scattering losses

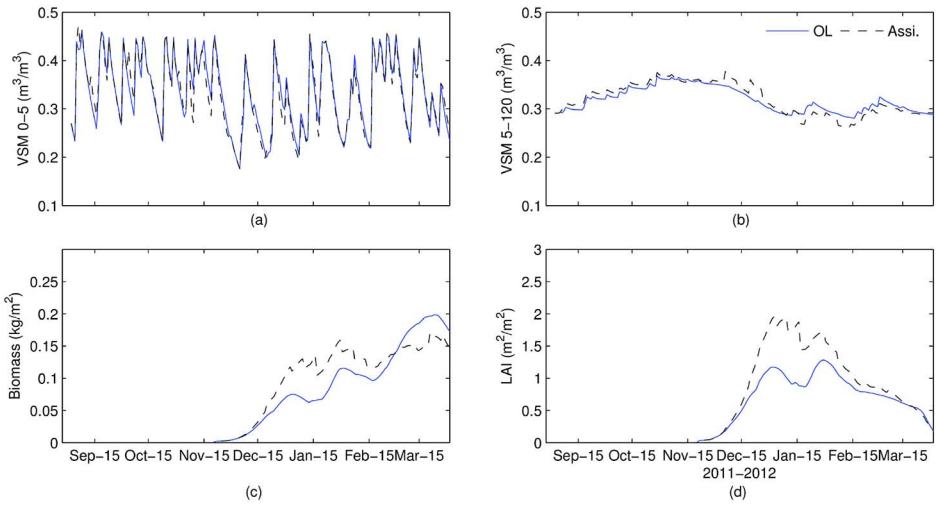

Fig. 7. Comparison of regionally-averaged open loop and assimilated estimates using Aquarius of (a) $VSM_{0-5\text{cm}}$; (b) $VSM_{5-120\text{cm}}$; (c) dry biomass; and (d) LAI.

TABLE VIII
RMSD AND ASD OF $VSM_{0-5\text{ cm}}$, $VSM_{0-120\text{ cm}}$, BIOMASS, AND LAI BETWEEN OPEN LOOP AND DATA ASSIMILATION USING AP OBSERVATIONS FROM AQUARIUS

	$VSM_{0-5\text{ cm}}$ (m^3/m^3)		$VSM_{5-120\text{ cm}}$ (m^3/m^3)		B_D (kg/m^2)		LAI (m^2/m^2)	
	RMSD	ASD	RMSD	ASD	RMSD	ASD	RMSD	ASD
Assi.	0.021	0.045	0.015	0.026	0.036	0.120	0.397	1.002

TABLE IX
MEAN AND STANDARD DEVIATION OF LAI FROM MODIS PRODUCT IN TWO PIXELS AND LAI FROM ASSIMILATION OF AQUARIUS AP OBSERVATIONS

Pixel	DAP 30 (Early-)			DAP 75 (Mid-)			DAP 125 (Reproductive)		
	MODIS		Aquarius	MODIS		Aquarius	MODIS		Aquarius
	Mean	SD	Assi.	Mean	SD	Assi.	Mean	SD	Assi.
1	0.80	0.38	0.67	1.31	0.62	1.64	0.91	0.38	0.50
2	0.73	0.38	0.60	1.91	0.93	1.61	0.80	0.37	0.76

Pixels 1 and 2 contain 9167 and 9278 agricultural LAI values, respectively, from MODIS.

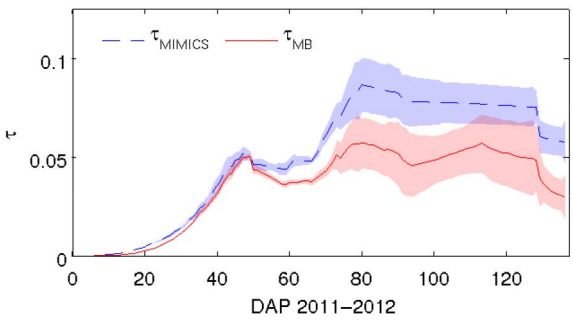

Fig. 8. Comparison of τ values in MIMICS and MB models. The bounded area represents one standard deviation of the two τ values.

are significant for passive signatures, particularly for the more structural plants such as trees [66]. The τ_{MB} would need to be modified to include scattering losses for realistic brightness predictions.

VI. SUMMARY AND CONCLUSION

In this study, a data assimilation framework that is capable of incorporating complementarities of AP observations was developed and implemented for updating SM at two layers and vegetation biomass through a growing season of soybean. Overall, estimates of SM, dry biomass, and LAI using the data assimilation framework were significantly improved in the synthetic experiments. Data assimilation conducted every 3 days showed more improvement than that conducted every 7 days in estimates of $SM_{0-5\text{ cm}}$ and dry biomass by 12% and 17%, respectively, indicating that the high temporal resolution observations are needed for such highly dynamic parameters. Although data assimilation every 3 days improved the estimation of dry biomass and LAI by as much as 42% and 20%, respectively, over the open loop, their ASDs were still higher. The wider spread of vegetation estimations resulted from the unrealistic estimate of vegetation development in some ensemble members using the uncalibrated DSSAT model in this study. A calibrated DSSAT model is recommended, so that the plant for each ensemble member is able to adapt to the meteorological and hydrological conditions in this region. In addition, further study on developing a backscatter model that involves the contribution from pods is suggested in order to improve estimates during the reproductive period.

The LAI estimate based on assimilating Aquarius observations was compared to the MODIS LAI product averaged to a 100-km scale. Even though the MODIS products may contain errors, in the absence of ground truth, the comparison showed that the LAI from data assimilation is of a similar quality as MODIS products, which have been widely used on monitoring vegetation growth. However, for agricultural use, observations with better spatial resolutions are recommended. This study also showcased the potential ability of the SMAP mission that provides better temporal and spatial resolutions of synchronous AP observations for improved estimates of SM and vegetation parameters during the dynamic agricultural growing season. In addition, investigation of impacts due to inconsistent vegetation opacities in backscatter and MB models on performance of assimilation is recommended for improving the assimilation algorithm.

ACKNOWLEDGMENT

The authors thank the anonymous reviewers for providing insightful comments and suggestions to improve the manuscript.

REFERENCES

[1] J. Jones *et al.*, "The DSSAT cropping system model," *Eur. J. Agron.*, vol. 18, nos. 3–4, pp. 235–265, 2003.

[2] B. Ruiz-Nogueira, K. Boote, and F. Sau, "Calibration and use CROPGRO-soybean model for improving soybean management under rainfed conditions," *Agric. Syst.*, vol. 68, pp. 151–173, 2001.

[3] J. Judge, "Microwave remote sensing of soil water: Recent advances and issues," *Trans. Amer. Soc. Agric. Biol. Eng.*, vol. 50, no. 5, pp. 1645–1649, 2007.

[4] A. de Wit and C. van Diepen, "Crop model data assimilation with ensemble Kalman filter for improving regional crop yield forecasts," *Agric. For. Meteorol.*, vol. 146, pp. 38–56, 2007.

[5] L. Prévot, H. Chauki, D. Troufleau, M. Weiss, and N. B. F. Baret, "Assimilating optical and radar data into the STICS crop model for wheat," *Agron. Sustain. Dev.*, vol. 23, no. 4, pp. 297–303, 2003.

[6] J.-C. Calvet, J.-P. Wigneron, J. Walker, F. Karbou, A. Chanzy, and C. Albergel, "Sensitivity of passive microwave observations to soil moisture and vegetation water content: L-band to W-band," *IEEE Trans. Geosci. Remote Sens.*, vol. 49, no. 4, pp. 1190–1199, Apr. 2011.

[7] D. Entekhabi *et al.*, "The soil moisture active passive (SMAP) mission," *Proc. IEEE*, vol. 98, no. 5, pp. 704–716, May 2010.

[8] Y. Kerr *et al.*, "The SMOS mission: New tool for monitoring key elements of the global water cycle," *Proc. IEE*, vol. 98, no. 5, pp. 666–687, May 2010.

[9] D. Le Vine, G. Lagerloef, F. Colomb, S. Yueh, and F. Pellerano, "Aquarius: An instrument to monitor sea surface salinity from space," *IEEE Trans. Geosci. Remote Sens.*, vol. 45, no. 7, pp. 2040–2050, Jul. 2007.

[10] R. Bindlish, T. Jackson, M. Cosh, T. Zhao, and P. O'Neill, "Global soil moisture from the Aquarius/SAC-D satellite: Description and initial assessment," *IEEE Geosci. Remote Sens. Lett.*, vol. 12, no. 5, pp. 923–927, May 2015.

[11] J.-P. Wigneron *et al.*, "Evaluating an improved parameterization of the soil emission in L-MEB," *IEEE Trans. Geosci. Remote Sens.*, vol. 49, no. 4, pp. 1177–1189, Apr. 2011.

[12] T. Jackson, "Measuring surface soil moisture using passive microwave remote sensing," *Hydrol. Process.*, vol. 7, no. 2, pp. 139–152, 1993.

[13] L. Pasolli *et al.*, "Estimation of soil moisture in mountain areas using SVR technique applied to multiscale active radar images at C-band," *IEEE J. Sel. Topics Appl. Earth Observ. Remote Sens.*, vol. 8, no. 1, pp. 262–283, Jan. 2015.

[14] S. Paloscia, P. Pampaloni, and E. Santi, "A comparison of algorithms for retrieving soil moisture from ENVISAT/ASAR images," *IEEE Trans. Geosci. Remote Sens.*, vol. 46, no. 10, pp. 3274–3284, Oct. 2008.

[15] C. Notarnicola, M. Angiulli, and F. Posa, "Use of a radar and optical remotely sensed data for soil moisture retrieval on vegetated areas," *IEEE Trans. Geosci. Remote Sens.*, vol. 44, no. 4, pp. 925–935, Apr. 2006.

[16] O. Merlin, A. Chehbouni, G. Boulet, and Y. Kerr, "Assimilation of disaggregated microwave soil moisture into a hydrologic model using coarse-scale meteorological data," *J. Hydrometeorol.*, vol. 7, no. 6, pp. 1308–1322, 2006.

[17] A. Monsivais-Huertero, W. Graham, J. Judge, and D. Agrawal, "Effect of simultaneous state-parameter estimation and forcing uncertainties on root-zone soil moisture for dynamic vegetation using ENKF," *Adv. Water Resour.*, vol. 33, no. 4, pp. 468–484, 2010.

[18] C. Draper, R. Reichle, G. D. Lannoy, and Q. Liu, "Assimilation of passive and active soil moisture retrievals," *Geophys. Res. Lett.*, vol. 30, pp. 1–5, 2012, L04401, doi:10.1029/2011GL050655.

[19] A. Ines, N. Das, J. Hansen, and E. Njoku, "Assimilation of remotely sensed soil moisture and vegetation with a crop simulation model for maize yield prediction," *Remote Sens. Environ.*, vol. 138, pp. 149–164, 2013.

[20] S. Chakrabarti, T. Bongiovanni, J. Judge, L. Zotarelli, and C. Bayer, "Assimilation of SMOS soil moisture for quantifying drought impacts on crop yield agricultural regions," *IEEE J. Sel. Topics Appl. Earth Observ. Remote Sens.*, vol. 7, no. 9, pp. 3867–3879, Sep. 2014.

[21] K. Nagarajan, J. Judge, A. Monsivais-Huertero, and W. Graham, "Impacts of assimilation passive microwave observations on root-zone soil moisture under dynamic vegetation conditions," *IEEE Trans. Geosci. Remote Sens.*, vol. 50, no. 11, pp. 4279–4291, Nov. 2012.

[22] Y. Du, F. Ulaby, and M. Dobson, "Sensitivity to soil moisture by active and passive microwave sensors," *IEEE Trans. Geosci. Remote Sens.*, vol. 38, no. 1, pp. 105–114, Jan. 2000.

[23] P. O'Neill, N. Chauhan, and T. Jackson, "Use of active and passive microwave remote sensing for soil moisture estimation through corn," *Int. J. Remote Sens.*, vol. 17, no. 10, pp. 1851–1865, Jul. 1996.

[24] S. Dunne and D. Entekhabi, "Impact of multiresolution active and passive microwave measurements on soil moisture estimation using the ensemble kalman smoother," *IEEE Trans. Geosci. Remote Sens.*, vol. 45, no. 4, pp. 1016–1028, Apr. 2007.

[25] J. Oades and A. Waters, "Aggregate hierarchy in soils," *Aust. J. Soils Res.*, vol. 29, no. 6, pp. 815–828, 1991.

[26] J. Fan and I. Gijbels, L*ocal Polynomial Modelling and Its Applications: Monographs on Statistics and Applied Probability*. Boca Raton, FL, USA: CRC Press, vol. 66, 1996.

[27] K. Boote, J. Jones, G. Hoogenboom, and G. Wilkerson, *Evaluation of the CROPGRO-Soybean Model Over a Wide Range of Experiments*. Norwell, MA, USA: Kluwer, 1997.

[28] K. Boote and J. Jones, *Simulation of Crop Growth*. New York, NY, USA: Marcel Dekker, 1998.

[29] S. Jagtap and J. Jones, "Adaptation and evaluation of the cropgro-soybean model to predict regional yield and production," *Agric. Ecosyst. Environ.*, vol. 93, pp. 73–85, 2002.

[30] T. Mavromatis, K. Boote, W. James, G. Wilkerson, and G. Hoogenboom, "Repeatability of model genetic coefficients derived from soybean performance trials across different states," *Crop Sci.*, vol. 42, pp. 76–89, 2002.

[31] J. Dardanelli, M. Calmon, J. Jones, J. Andriani, M. Diaz, and D. Collino, "Use of a crop model to evaluate soil impedance and root clumping effects on soil water extraction in three argentine soils," *Trans ASAE*, vol. 46, no. 4, pp. 1265–1275, 2003.

[32] R. Braga and J. Jones, "Using optimization to estimate soil inputs of crop models for use in site-specific management," *Trans ASAE*, vol. 47, no. 5, pp. 1821–1831, 2004.

[33] J. Lizaso, W. Batchelor, K. Boote, M. Westgate, P. Rochette, and A. Moreno-Sotomayor, "Evaluating a leaf-level canopy assimilation model linked to ceres-maize," *J. Agron.*, vol. 97, pp. 734–740, 2005.

[34] G. Alagarswamy, K. Boote, L. Allen, and J. Jones, "Evaluating the cropgro-soybean model ability to simulate photosynthesis response to carbon dioxide levels," *J. Agron.*, vol. 93, pp. 34–42, 2006.

[35] J. Timsina, K. Boote, and S. Duffield, "Evaluating the cropgro soybean model for predicting impacts of insect defoliation and depodding," *J. Agron.*, vol. 99, pp. 148–157, 2007.

[36] J. Ritchie, "A user-oriented model of the soil water balance in wheat," in *Wheat Growth and Modelling*, NATO-ASI Sciences-Series A: Life Sciences. New York, NY, USA: Springer, vol. 86, 1985, pp. 283–305.

[37] K. E. Saxton, W. Rawls, J. Romberger, and R. Papendick, "Estimating generalized soil-water characteristics from texture," *Soil Sci. Soc. Amer. J.*, vol. 50, pp. 1031–1036, 1986.

[38] A. Pires and M. Mattiazzo, "Kinetics of heavy metal solubilization by organic acids in sludge-treated soils," *Rev. Bras. Ciência Solo*, vol. 31, pp. 143–151, 2007.

[39] L. Chig, E. Couto, J. Novaes Filho, L. Rodrigues, M. Johnson, and O. Weber, "Spatial distribution of soil texture, color and soil organic carbon across a headwater transect in the southern amazon," *Acta Amazonica*, vol. 38, pp. 715–722, 2008.
[40] J. Marquesi, W. Teixeira, A. Reis, O. Cruz Junior, S. Batista, and M. Afonso, "Chemical, physical and hydric attributes and mineralogy of clay fractions in soils of lower amazon: Serra de parintins," *Acta Amazonica*, vol. 40, pp. 1–12, 2010.
[41] M. Campos, M. Ribeiro, V. Souza Júnior, M. Ribeiro Filho, and R. Souza, "Soil-landscape relationships on a granite substrate toposequence in santo antônio do matupi, manicoré, amazonas," *Rev. Bras. Ciência Solo*, vol. 35, pp. 13–23, 2011.
[42] A. Genú and J. Demattê, "Spectroradiometry of soil and comparison with orbital sensors," *Bragantia*, vol. 71, pp. 82–89, 2012.
[43] K. Chen, T. Wu, L. Tsang, Q. Li, J. Shi, and A. Fung, "Emission of rough surfaces calculated by the integral equation method with comparison to three-dimensional moment method simulations," *IEEE Trans. Geosci. Remote Sens.*, vol. 41, no. 1, pp. 90–101, Jan. 2003.
[44] V. Mironov, L. Kosolapova, and S. Fomin, "Physically and mineralogically based spectroscopic dielectric model for moist soils," *IEEE Trans. Geosci. Remote Sens.*, vol. 47, no. 7, pp. 2059–2070, Jul. 2009.
[45] F. Ulaby, K. Sarabandi, K. McDonal, M. Whitt, and M. Dobson, "Michigan microwave canopy scattering model (MIMICS)," *Int. J. Remote Sens.*, vol. 11, no. 7, pp. 1223–1253, Jul. 1990.
[46] A. Toure, K. Thomson, G. Edwards, R. Brown, and B. Brisco, "Adaptation of the MIMICS backscattering model to the agricultural context-wheat and canola at L and C bands," *IEEE Trans. Geosci. Remote Sens.*, vol. 32, no. 1, pp. 47–61, Jan. 1994.
[47] J.-P. Wigneron, P. Ferrazzoli, J.-C. Calvet, Y. Kerr, and P. Bertuzzi, "A parametric study on passive and active microwave observations over a soybean crop," *IEEE Trans. Geosci. Remote Sens.*, vol. 37, no. 6, pp. 2728–2733, Nov. 1999.
[48] R. De Roo, Y. Du, F. Ulaby, and M. Dobson, "A semi-empirical backscattering model at L-band and C-band for a soybean canopy with soil moisture inversion," *IEEE Trans. Geosci. Remote Sens.*, vol. 39, no. 4, pp. 864–872, Apr. 2001.
[49] S.-B. Kim, M. Moghaddam, L. Tsang, M. Burgin, X. Xu, and E. Njoku, "Models of L-band radar backscattering coefficients over global terrain for soil moisture retrieval," *IEEE Trans. Geosci. Remote Sens.*, vol. 52, no. 2, pp. 1381–1396, Feb. 2014.
[50] A. Kenig *et al.*, "Development of soybean fresh and SRY weight relationship for real time model calibration," *Agron. J.*, vol. 85, no. 1, pp. 140–146, 1993.
[51] W. Fehr and C. Caviness, "Stages of soybean development," Cooperative Extension Serv., Agric. Home Econ. Exp. Station, Iowa State Univ., Ames, IA, USA, Special Report 80, 1977 [Online]. Available: http://www.agencia.cnptia.embrapa.br/Repositorio/STAGES.+FEHR_000g50w2l4s02wx5ok0dkla0sik2sqav.pdf
[52] W. Burke, T. Schmugge, and J. Paris, "Comparison of 2.8- and 21-cm microwave radiometer observations over soils with emission model calculations," *J. Geophys. Res.*, vol. 84, no. C1, pp. 287–294, 1979.
[53] J. Casanova, J. Judge, and M. Jang, "Modeling transmission of microwaves through dynamic vegetation," *IEEE Trans. Geosci. Remote Sens.*, vol. 45, no. 10, pp. 3145–3149, Oct. 2007.
[54] J. Patton and B. Hornbuckle, "Initial validation of SMOS vegetation optical thickness in Iowa," *IEEE Geosci. Remote Sens. Lett.*, vol. 10, no. 4, pp. 647–651, Jul. 2013.
[55] D. Entekhabi, N. Das, E. Njoku, J. Johnson, and J. Shi, "Algorithm theoretical basis document L2 & L3 radar/radiometer soil moisture (Active/Passive) data products: Initial release, v.1," Jet Propul. Lab., California Inst. Technol., Tech. Rep. D-66481, 2012 [Online]. Available: http://nsidc.org/data/smap/pdfs/atbds/l2&3_sm_ap_initrel_v11_6.pdf
[56] A. Gelb, *Applied Optimal Estimation*. Cambridge, MA, USA: MIT Press, 1974.
[57] G. Evensen, "The ensemble Kalman filter: Theoretical formulation and practical implementation," *Ocean Dyn.*, vol. 53, no. 4, pp. 343–367, 2003.
[58] L. Zotarelli *et al.*, "Influence of no-tillage and frequency of a green manure legume in crop rotations for balancing N outputs and preserving soil organic C stocks," *Field Crop Res.*, vol. 132, no. 14, pp. 185–195, 2012.
[59] T. Bongiovanni *et al.*, "Field observations during the ninth microwave, water, and energy balance experiment (MicroWEX-9): From March 24,2010through January 6, 2011," Center Remote Sens., Univ. Florida, Gainesville, FL, USA, Tech. Rep. AE494, 2012 [Online]. Available: http://edis.ifas.ufl.edu/pdffiles/AE/AE49400.pdf
[60] M. Piles, D. Entekhabi, and A. Camps, "A change detection algorithm for retrieving high-resolution soil moisture from SMAP radar and radiometer observations," *IEEE Trans. Geosci. Remote Sens.*, vol. 47, no. 12, pp. 4125–4131, Dec. 2012.
[61] A. Sahoo, C. D. Lannoy, R. Reichle, and P. Houser, "Assimilation and downscaling of satellite observed soil moisture over the littel river experiment watershed in Georgia, USA," *Adv. Water Resour.*, vol. 52, pp. 19–33, 2013.
[62] S. Kumar, R. Reichle, K. W. Harrison, C. Peter-Lidard, S. Yatheendradas, and J. Santanello, "A comparison of methods for a prior bias correction in soil moisture data assimilation," *Water Resour. Res.*, vol. 48, no. W03515, pp. 1–16, 2012, doi: 10.1029/2010WR010261.
[63] J.-C. L. Lukeba, R. Vumilia, K. Nkongolo, M. Mwabila, and M. Tsumbu, "Growth and leaf area index simulation in Maize (Zea mays L.) under small-scale farm conditions in a sub-Saharan African region," *Amer. J. Plant Sci.*, vol. 4, pp. 575–583, 2013.
[64] Z. Li, H. Tang, X. Xin, B. Zhang, and D. Wang, "Assessment of the MODIS product using ground measurement data and HJ-1A/1B imagery in the meadow steppe of Hulunber, China," *Remote Sens.*, vol. 6, pp. 6242–6263, 2014.
[65] R. Myneni *et al.*, "Global products of vegetation leaf area and fraction absorbed PAR from year one of MODIS data," *Remote Sens. Environ.*, vol. 83, pp. 214–231, 2002.
[66] P. Ferrazzoli, L. Guerriero, and J.-P. Wigneron, "Simulating L-band emission of forests in view of future satellite applications," *IEEE Trans. Geosci. Remote Sens.*, vol. 40, no. 12, pp. 2700–2708, Dec. 2002.

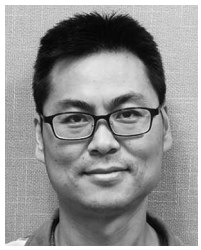

Pang-Wei Liu (S'09–M'13) received the Ph.D. degree in agricultural engineering with a minor in electrical engineering from the University of Florida, Gainesville, FL, USA, in 2013.

Currently, he is a Postdoctoral Research Associate with the Center for Remote Sensing, Institute of Food and Agricultural Sciences, University of Florida. His research interests include active and passive microwave remote sensing modeling for soil moisture and agricultural crops under dynamic vegetation conditions; data assimilation with crop growth models; application of LiDAR for forest biomass; and GNSS-R remote sensing for terrestrial applications.

Dr. Liu is a member of the IEEE-GRSS and American Geophysical Union.

Tara Bongiovanni received the B.S. and M.E. degrees in agricultural and biological engineering from the University of Florida, Gainesville, FL, USA, in 2009 and 2012, respectively. Her Master's research focused on modeling crop growth and development and on improving modeled estimates of biomass and yield through assimilating remote sensing observations.

Currently, she is working with the Center of Remote Sensing, University of Florida. Her research interests include GIS work for decision support models, which includes processing field and remotely sensed data, also she supervises crop vegetation sampling, data collection, sensor monitoring, and data archiving for the Center.

Alejandro Monsivais-Huertero (S'06–M'07–SM'13) received the B.S. degree in telecommunications engineering from the National Autonomous University of Mexico, Mexico City, Mexico, in 2002, and the M.S. degree in microwaves and optical telecommunications and the Ph.D. degree in microwaves, electromagnetism, and optoelectronics from the University of Toulouse, Toulouse, France, in 2004 and 2007, respectively.

From 2004 to 2006, he was with the Antennes, Dispositifs et Materiaux Microondes Laboratory, and from 2006 to 2007, with the Laboratoire dEtudes et de Recherche en Imagerie Spatiale et Medicale, both at the University of Toulouse. From 2008 to 2009, he was as a Postdoctoral Research Associate with the Center for Remote Sensing, Department of Agricultural and Biological Engineering, University of Florida, Gainesville, FL, USA. Since 2010, he has been working as a Researcher with the Superior School of Mechanical and Electrical Engineering Campus Ticoman, National Polytechnic Institute of Mexico, Mexico City, Mexico. His research interests include in microwave and millimeter-wave radar remote sensing, electromagnetic wave propagation, and retrieval algorithms

Jasmeet Judge (S'94–M'00–SM'05) received the Ph.D. degree in electrical engineering and atmospheric, oceanic, and space sciences from the University of Michigan, Ann Arbor, MI, USA, in 1999.

Currently, she is the Director of the Center for Remote Sensing and an Associate Professor in the Agricultural and Biological Engineering Department, Institute of Food and Agricultural Sciences, University of Florida, Gainesville, FL, USA. Her research interests include microwave remote sensing applications to terrestrial hydrology for dynamic vegetation; data assimilation; modeling of energy and moisture interactions at the land surface and in the vadose zone; and spatio-temporal scaling of remotely sensed observations in heterogenous landscapes.

Dr. Judge is the Chair of the National Academies Committee on Radio Frequencies and a member of the Frequency Allocations in Remote Sensing Technical Committee in the IEEE-GRSS.

Susan Steele-Dunne received the S.M. and Ph.D. degrees in hydrology from Massachusetts Institute of Technology, Cambridge, MA, USA, in 2002 and 2006, respectively. Since 2008, she has been with the Water Resources Section, Faculty of Civil Engineering and Geosciences, Delft University of Technology, Delft, The Netherlands.

Her research interests include remote sensing, data assimilation, land atmosphere interactions, and land surface modeling.

Dr. Steele-Dunne is a member of the American Meteorological Society and the American Geophysical Union. She has also served the American Geophysical Union Hydrology Section as a member of the Remote Sensing Technical Committee and the Hydrological Sciences Award Committee, and the American Meteorological Society as a member of the Hydrology Committee.

Rajat Bindlish (S'98–M'01–SM'05) received the B.S. in civil engineering from Indian Institute of Technology Bombay, Mumbai, India, in 1993, and the M.S. and Ph.D. degrees in civil engineering from Pennsylvania State University, State College, PA, USA, in 1996 and 2000, respectively.

Currently, he is with Science Systems and Applications, Inc. (SSAI), U.S. Department of Agriculture, Agricultural Research Service, Hydrology, and Remote Sensing Laboratory, Beltsville, MD, USA. Currently, he is working on soil moisture estimation from microwave sensors and their subsequent application in land surface hydrology. His research interests include the application of microwave remote sensing in hydrology.

Thomas J. Jackson (SM'96–F'02) received the Ph.D. degree in civil engineering from the University of Maryland, College Park, MD, USA, in 1976.

He is a Research Hydrologist with the U.S. Department of Agriculture, Agricultural Research Service, Hydrology, and Remote Sensing Laboratory, Beltsville, MD, USA. His research interests include application and development of remote sensing technology in hydrology and agriculture, primarily microwave measurement of soil moisture.

Dr. Jackson is a Fellow of the Society of Photo-Optical Instrumentation Engineers, the American Meteorological Society, and the American Geophysical Union. He has been a member of the science and validation teams of the Aqua, ADEOS-II, Radarsat, Oceansat-1, Envisat, ALOS, SMOS, Aquarius, GCOM-W, and SMAP remote sensing satellites. In 2003, he was the recipient of the William T. Pecora Award (NASA and Department of Interior) for outstanding contributions toward understanding the Earth by means of remote sensing and the AGU Hydrologic Sciences Award for outstanding contributions to the science of hydrology. He was the recipient of the IEEE Geoscience and Remote Sensing Society Distinguished Achievement Award in 2011.